

Gwangju Institute of
Science and Technology

School of Electrical Engineering and Computer Science



Biomedical Image Processing and Analysis

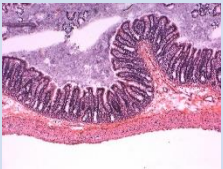
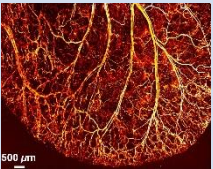


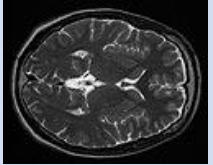
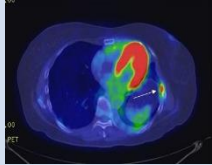
- *Ph.D. Dissertation Proposal* -

Author : Pavel Ni

Supervisor : Prof. Heung-No Lee

May 16, 2018

- Introduction

Modality	Optical	Photoacoustic	Ultrasound	CT	MRI	PET/CT
Images						
PROS	Real-time Contrast Resolution	Contrast Resolution	Availability Cost Real-time	Sensitivity Resolution	Sensitivity Resolution	Contrast Resolution
CONS	Depth	Depth Real-time	Contrast Speckle	Contrast Radiation	Cost Throughput	Cost Radiation Throughput
Resolution	0.1 μm	10 μm	0.3-3 mm	1 mm	1 mm	1 mm

- **Introduction**

- ***Computational Medical Imaging*** is a major area of interest because of its impact on quality of human life

Today, medical imaging research includes many different directions:

- Super-resolution
- Improved diagnostics using clinically meaningful information
- Multi-modal image fusion
- New algorithms for image analysis

Clinical analysis and medical intervention:

- Lesion detection
- Cancer therapy
- Activity estimation

Contributions of this Research

1. High-Resolution Sonography using Wave Interference
2. Compressive Sensing Reconstruction of Photoacoustic Images
3. Biomedical Image Processing and Analysis using Deep Neural Networks

Gwangju Institute of
Science and Technology

School of Electrical Engineering and Computer Science



1. High-Resolution Sonography using Wave Interference

1. High-Resolution Sonography using Wave Interference

• Introduction

- Ultrasound is a sound with a frequency between 1-20 MHz.
- Ultrasound imaging works according to the pulse-echo principle: a pulse is emitted by an array, the wave propagates and portion of its energy backscattered from the tissue.
- Ultrasound waves reflect at the borders between materials with different impedance.
- Received ultrasound signals are processed and displayed as a grayscale image.
- In conventional sonography, spatial resolution is achieved through focusing and steering of an ultrasound beam (delay-and-sum beamforming).

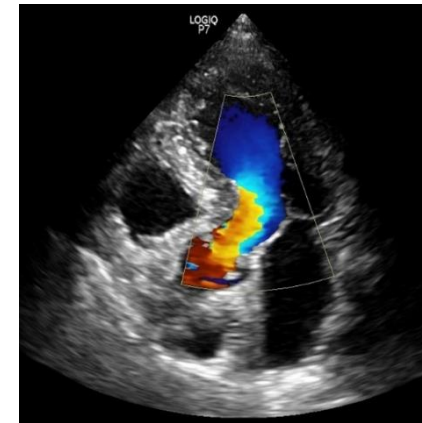


Fig. 1. Sonography

1. High-Resolution Sonography using Wave Interference

• Introduction

- Ultrasound is leading imaging modality worldwide
- Provides real-time images of anatomy and dynamic movement of organs
- Ultrasound can be used in diagnostic, therapy and surgical purposes.
- Cheap and portable
- Has many specific clinical applications:
 - Cardiac
 - Vascular
 - Musculoskeletal
 - Transorbital
 - Intraoperative
 - Oblation

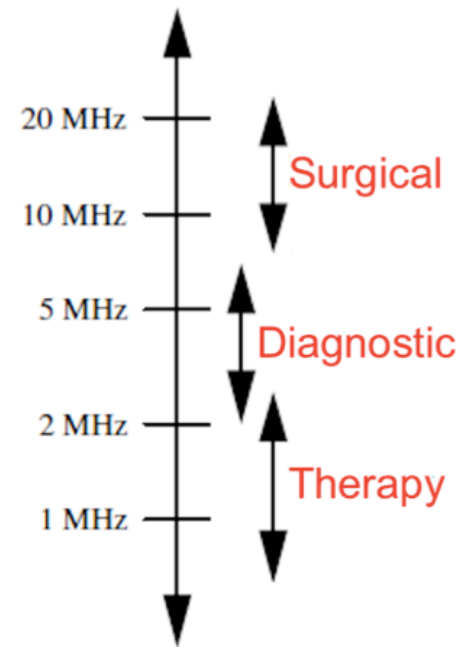


Fig. 2. Ultrasound applications

1. High-Resolution Sonography using Wave Interference

- **Background**

- Conventional ultrasound imaging methods are based on delay-and-sum beamforming.
- Beamforming is the process that used in array imaging, during which the received ultrasound signals are delayed and summed coherently.
- 2D Ultrasound images are obtained by using multiple focused pulse-echo transmissions.
- Spatial resolution in conventional ultrasound is limited due to acoustic diffraction.

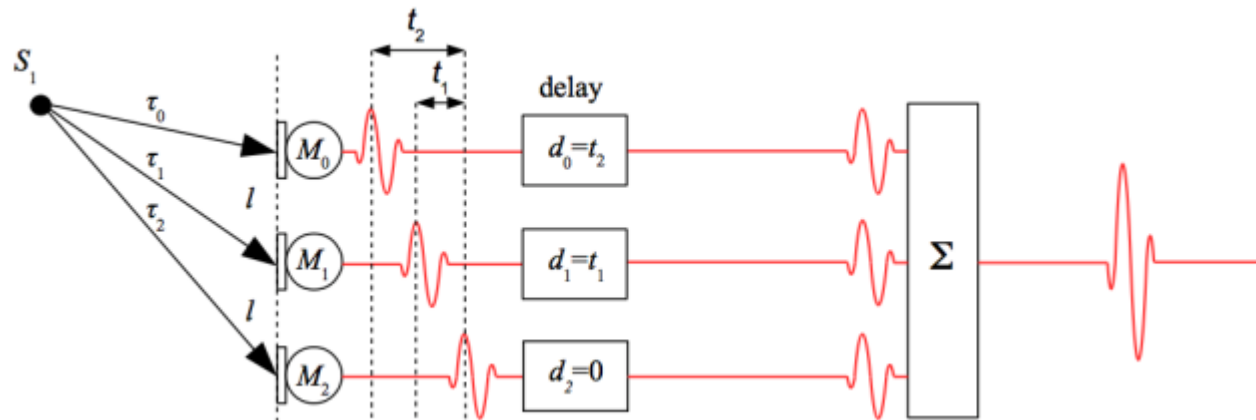


Fig. 3. Sonography

1. High-Resolution Sonography using Wave Interference

- Interference of ultrasound waves

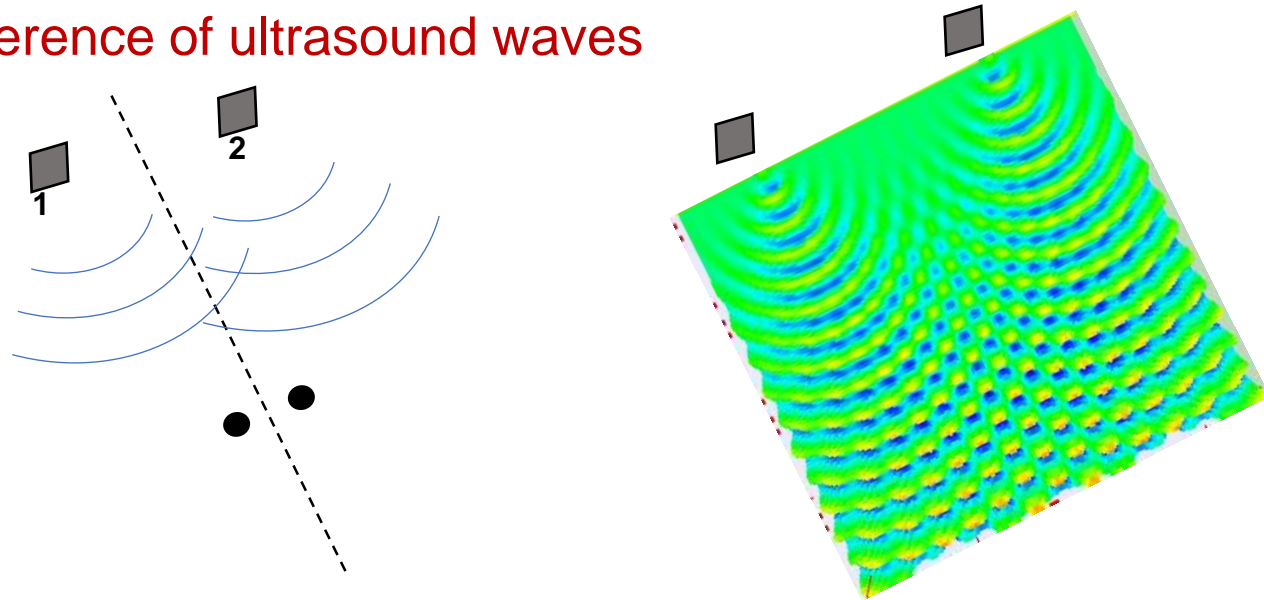


Fig. 4. Interference of waves

- We propose a method wherein the array elements are excited with randomly generated sequences, which yields a transmit ultrasound wavefront with a complex interference pattern
- Random interference patterns can be used to improve the resolution in ultrasound systems.

1. High-Resolution Sonography using Wave Interference

- **Sequence design**

- Random interference patterns can be generated electronically by using random excitation signals
- We generate a binary random sequence of length 8, where each element of the sequence is drawn from a set $\{-1, 1\}$ following the uniform distribution.
- Every element of the sequence convolved with the half cycle of a sine wave at a nominal frequency of 3 MHz.
- We can define random excitation sequences as

$$w_j(t) = \sum_{n=0}^{N-1} w[n] \delta\left(t - \frac{T}{2}(2n+1)\right) * \left[\cos\left(\pi \frac{t}{T}\right) * \text{rect}\left(\frac{t}{T}\right) \right], \quad (1)$$

- For example, w_j for $j = 1, 2$ is

$$\mathbf{w}_1 = (1, -1, 1, -1, 1, 1, -1, -1) \quad \text{and} \quad \mathbf{w}_2 = (1, -1, -1, -1, -1, 1, -1, 1)$$

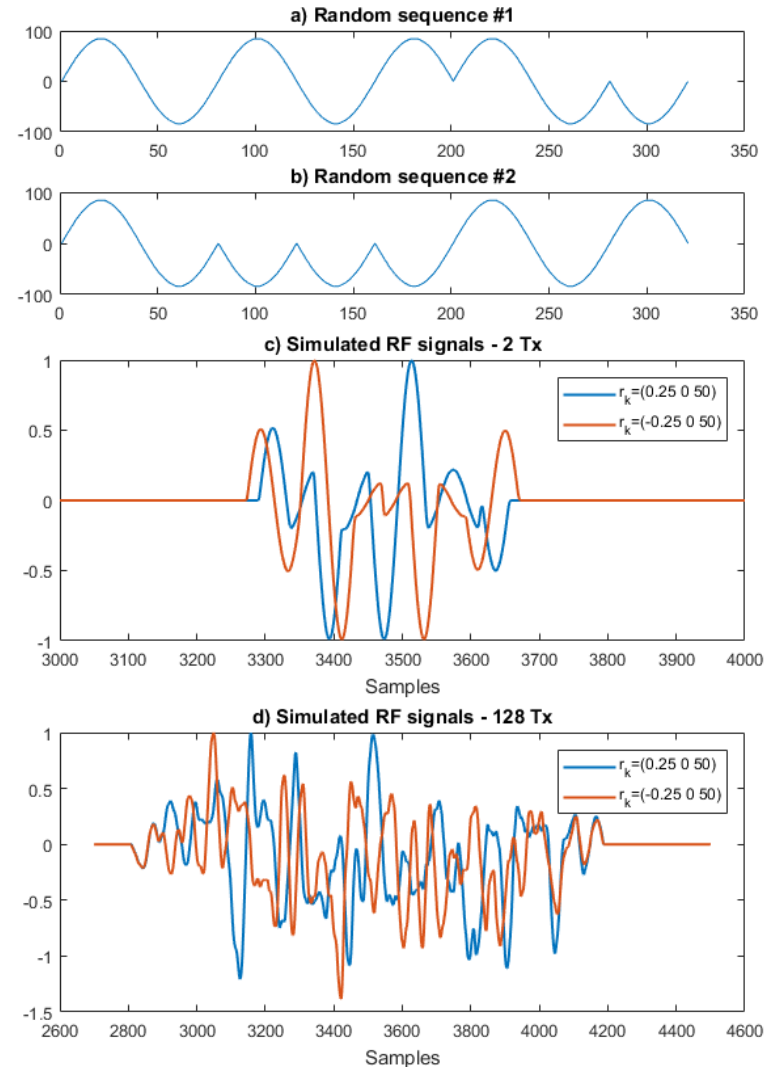


Fig. 5. a) and b) random excitation signals, c) Simulated impulse response of point targets when 2 array elements activated in transmission, d) Simulated impulse response when 128 array elements activated

1. High-Resolution Sonography using Wave Interference

- **Proposed method**

- We can model the received ultrasound signal as

$$p(\mathbf{r}_i, t) = E_m(t) \otimes_t \frac{1}{2} \int_{V'} F_{op} \left[\sum_{j=0}^{L-1} \rho_0 \frac{\partial w_j(t)}{\partial t} \otimes_t h_t(\mathbf{r}_k, \mathbf{r}_j, t) \right] \otimes_t h_r(\mathbf{r}_i, \mathbf{r}_k, t) d^3 \mathbf{r}_k, \quad (2)$$

Appendix A.

or in matrix and vector notation

$$\mathbf{p}_i = \mathbf{G}_i \mathbf{f}_i, \quad (3)$$

where $\mathbf{p}_i \in \mathbf{R}^M$ is a column vector representation of a raw ultrasound signal,

$\mathbf{f}_i \in \mathbf{R}^N$ is a vector representation of an ultrasound image,

the matrix $\mathbf{G}_i \in \mathbf{R}^{M \times N}$ is the transmission matrix.

Here, M is the number of measurements and N is the total number of point scatterers.

Ultrasound image \mathbf{f}_i can be reconstructed by finding the solution to the system of linear equations as follows

$$\min_{\mathbf{f} \in \mathbf{R}^n} \|\mathbf{f}_i\|_{w,1} + (1/\nu) \|\mathbf{G}_i \mathbf{f}_i - \mathbf{p}_i\|_1, \quad (4)$$

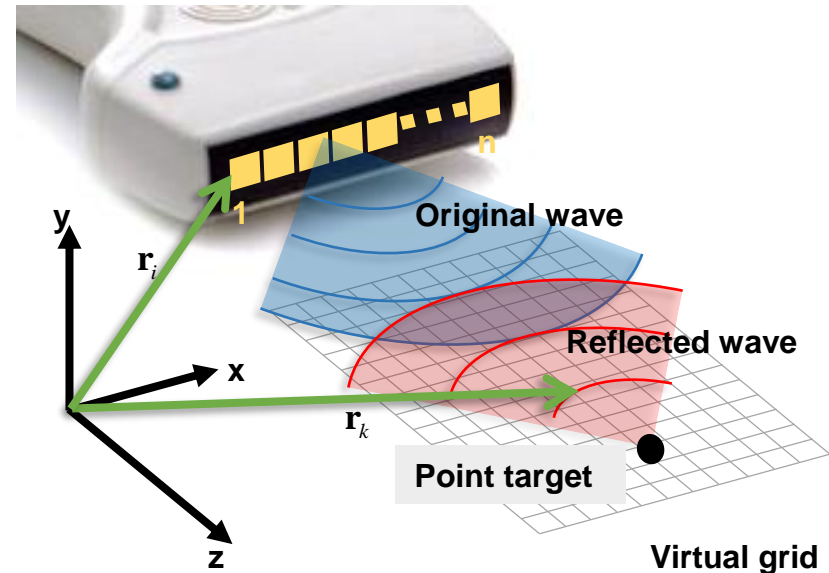


Fig. 6. Sonography

1. High-Resolution Sonography using Wave Interference

- Proposed method

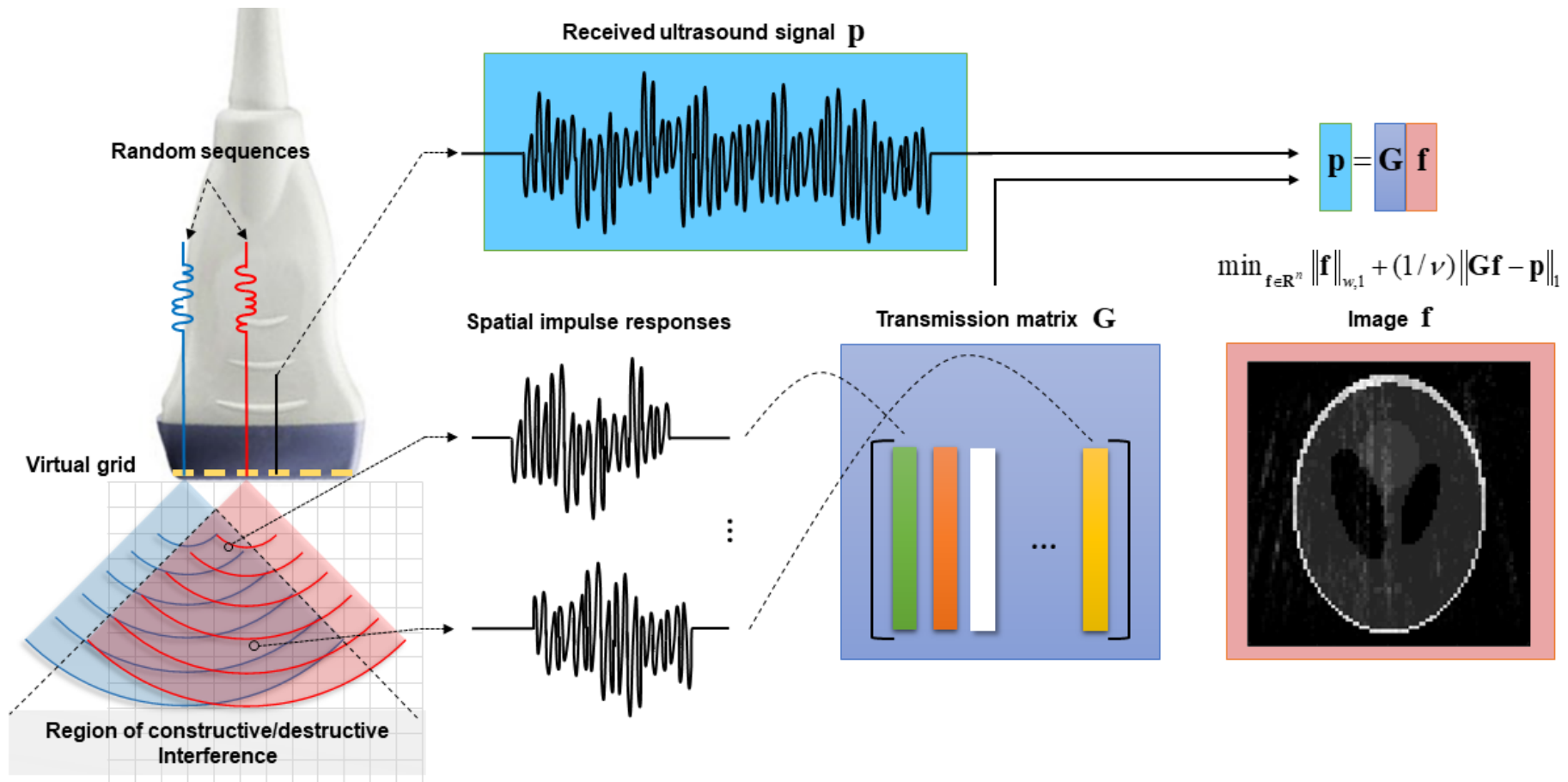


Fig. 7. Sonography

1. High-Resolution Sonography using Wave Interference

• Simulation Results

- A Shepp-Logan phantom is used to evaluate the reconstruction performance of the proposed method.
- In Fig. 9(e) we shown the intensity profiles of original scatterer map, image obtained using focused b-mode and the proposed method
- The proposed method can reconstruct location and intensity of scatterers much better then the conventional method.
- We achieved resolution of 0.25 mm which represents a four-fold improvement over conventional methods

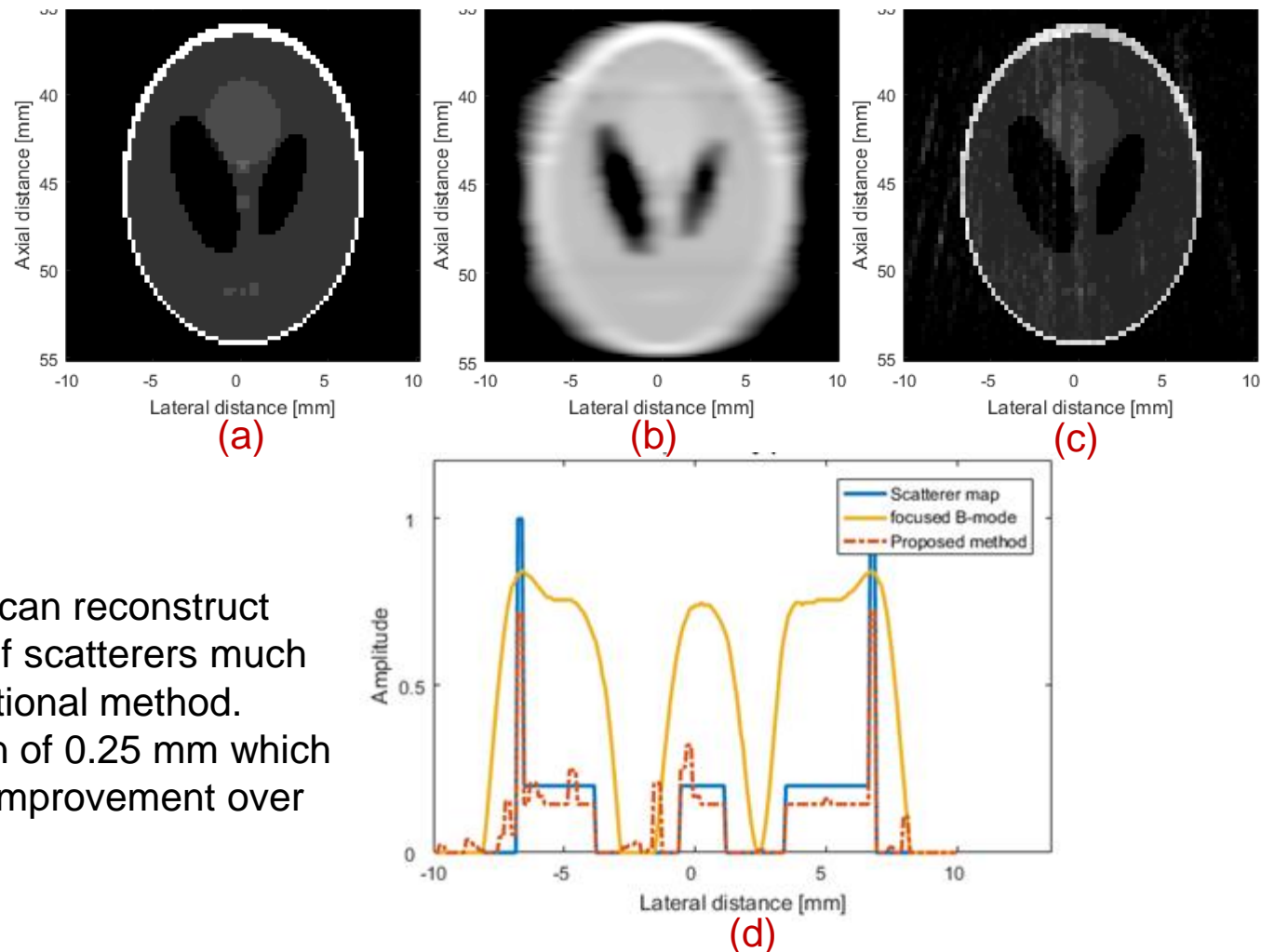


Fig. 8. Simulation results

1. High-Resolution Sonography using Wave Interference

• Experimental Results

- In order to verify our proposed method, we developed a research ultrasound system that is capable of generating a transmit ultrasound wavefront with spatially randomized interference patterns.
- The custom research setup is equipped with an arbitrary wave generator that has 128-cell memory for each transmit channel.
- The memory is used to store random excitation sequences of length 2048 of 8-bit data.
- The system features a linear transducer array with 128 piezo-electric crystals of 4.5-mm height and 0.3-mm width, which are separated by 0.03 mm from each other.

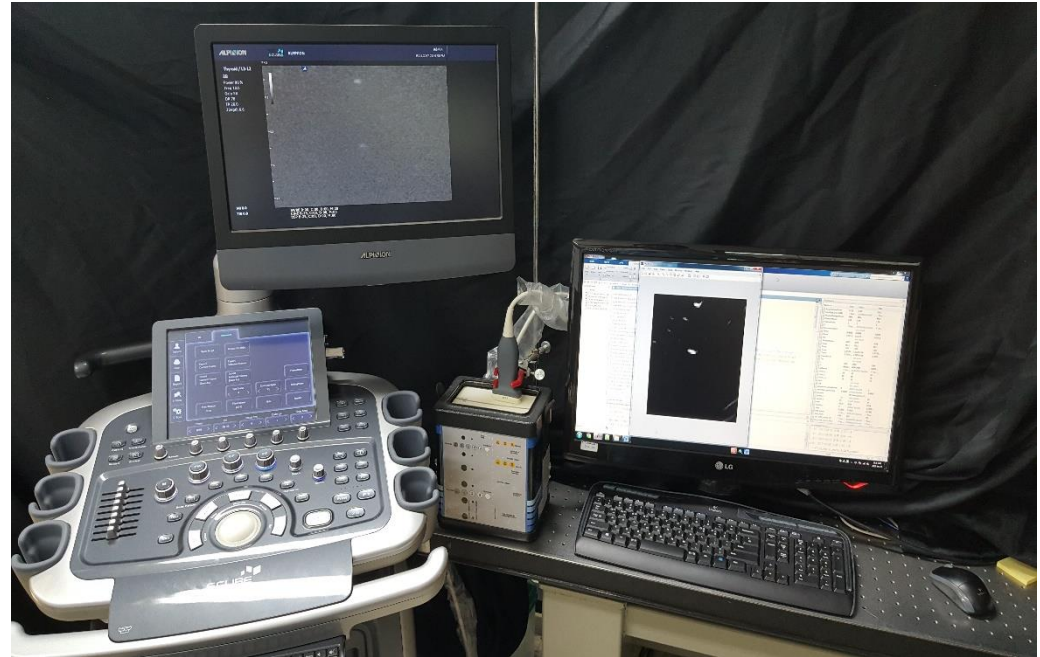
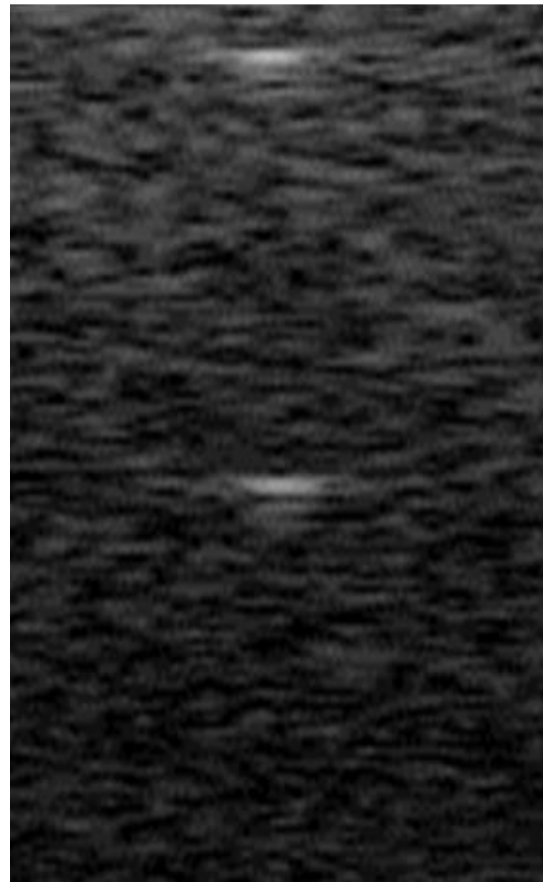


Fig. 9. Experimental setup

1. High-Resolution Sonography using Wave Interference

- **Experimental Results**

- In Fig. 10(a) the region of interest includes two nylon wires 100 μm in diameter located at depths of 40 mm and 50 mm from the transducer. A high-speckle region surrounds the nylon wires. Fig. 10(b) shows an ultrasound image reconstructed using the proposed interference based method, in which the two nylon wires can be clearly observed without any sidelobes or speckle noise.



(a)



(b)

Fig. 10. Experimental results. (a) an ultrasound image reconstructed using the conventional B-mode method with 256 scanlines (b) an image reconstructed using the proposed method

1. High-Resolution Sonography using Wave Interference

- Results

Parameters	INTERFERENCE BASED SONOGRAPHY (PROPOSED METHOD)	N. Wagner	Liu J	G. David	P. Krusinga
Tx scheme	- 1 firing of unfocused random wavefront - Excitation random sequence - 128 channels	- Focused transmission - 120 pulse-echo transmissions	- 32 firings of randomly apodized excitation - 128-channels	- 1 plane-wave - 128-channels	- Rotating single element with random mask - 72 Tx positions
Rx scheme	- Unfocused 26 channels	- 64 channels	- Full STA algorithm		- 72 Rx positions
Central Frequency	- 3 MHz	- 3.5 MHz	- 7.5 MHz	- 7.3 MHz	- 5 MHz
Number of CS problems	- 26	- 7,680	- 16,384	~	- 72
Spatial resolution	- 0.25 mm -	- 0.44 mm -	- 0.43 mm -	- 0.1 mm -	~
Results	- High contrast and detailed resolution for sparse and non-sparse objects	- 8-fold down-sampling	- Increased frame rate	- High resolution for sparse targets	- Single element imaging

1. High-Resolution Sonography using Wave Interference

- Summary

- We eliminated the need to focus and steer an ultrasound pulse, therefore, removed imposed resolution limit.
- Ultrasound image can be reconstructed using a single pulse-echo transmission which yields high-frame rate.
- When evaluated at the central frequency of 3 MHz, the proposed method results in a spatial resolution of 0.25 mm. Implying a four-fold improvement over the conventional methods.

1. High-Resolution Sonography using Wave Interference

- Future work

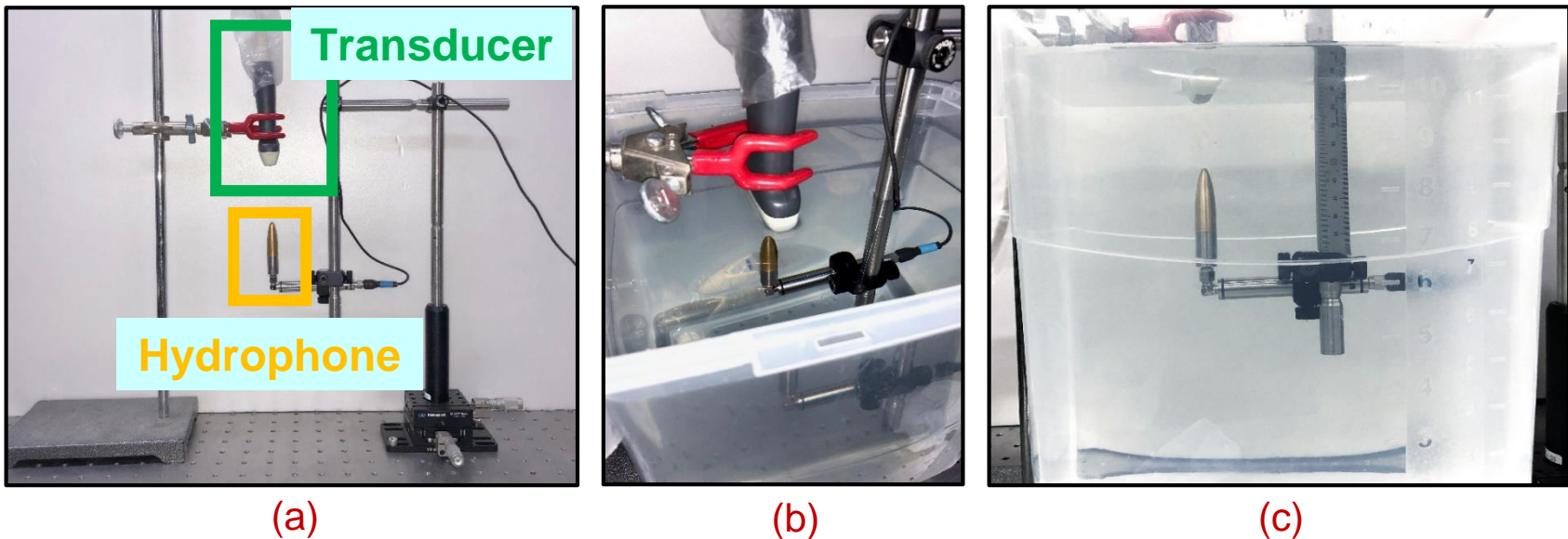


Fig. 11. Future experimental setup using hydrophone

- In order to successfully use the proposed method to screen human patients a more accurate transmission matrix is required.
- Transmission matrix can be designed using measurements from hydrophone and 3D scanning stage.

1. High-Resolution Sonography using Wave Interference

- Future work

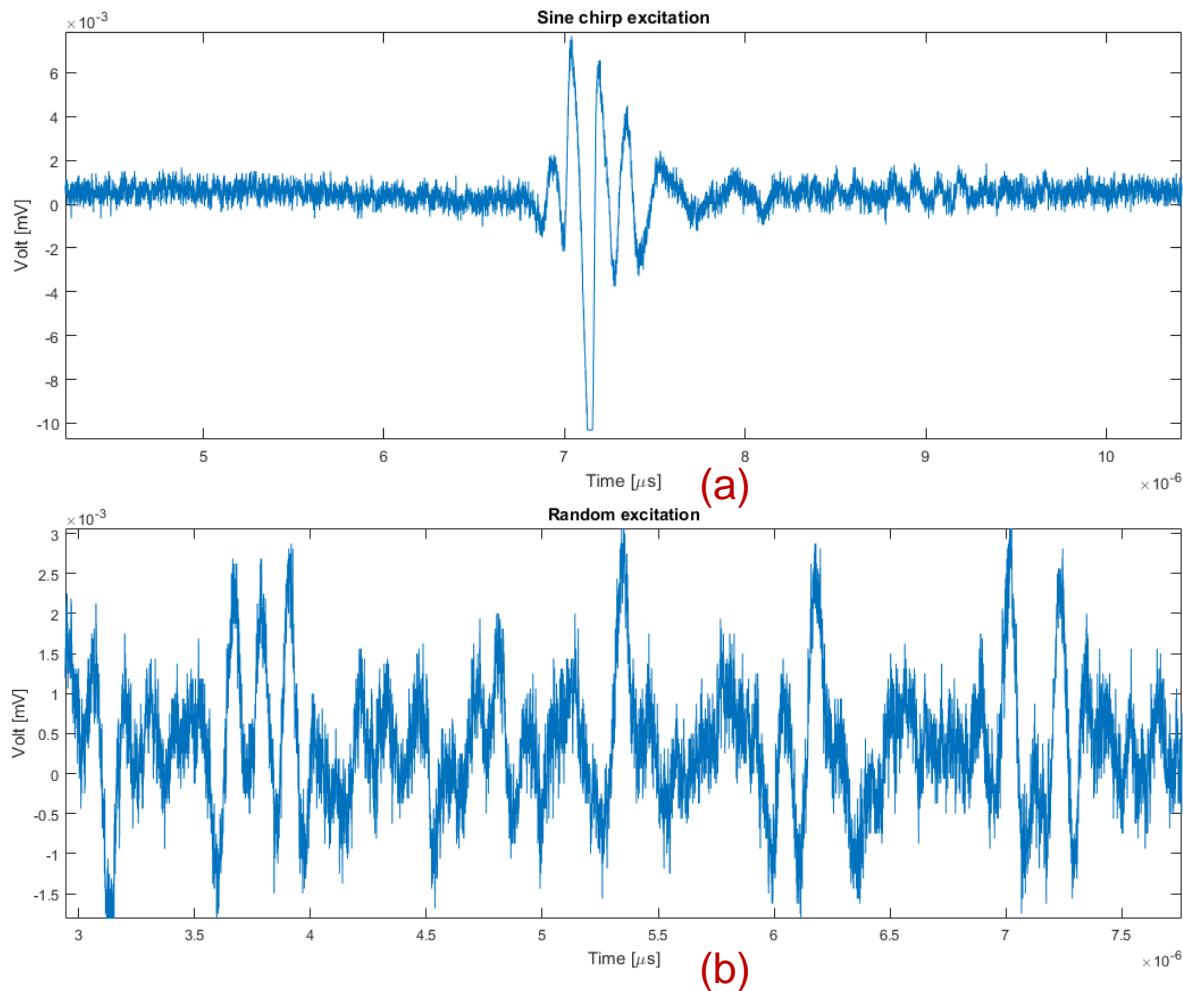


Fig. 12. Spatial impulse responses measured using hydrophone.

Gwangju Institute of
Science and Technology

School of Electrical Engineering and Computer Science

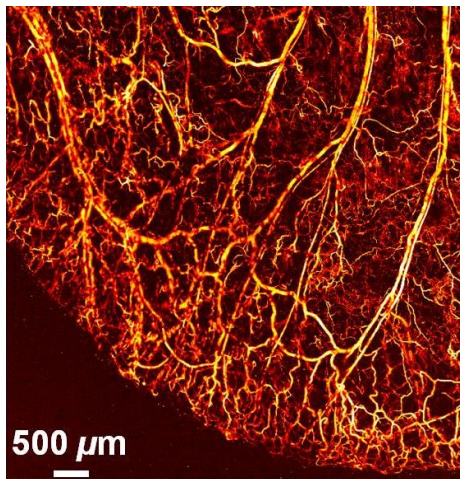


2. Photoacoustic Image Reconstruction using Compressive Sensing

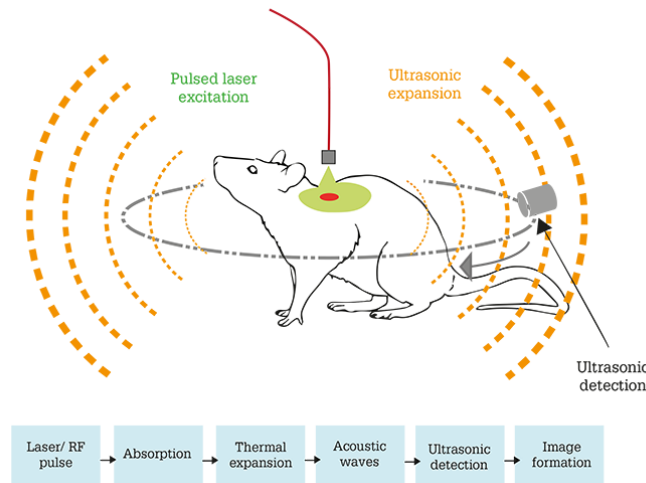
2. Compressive Sensing Reconstruction of Photoacoustic images

• Introduction

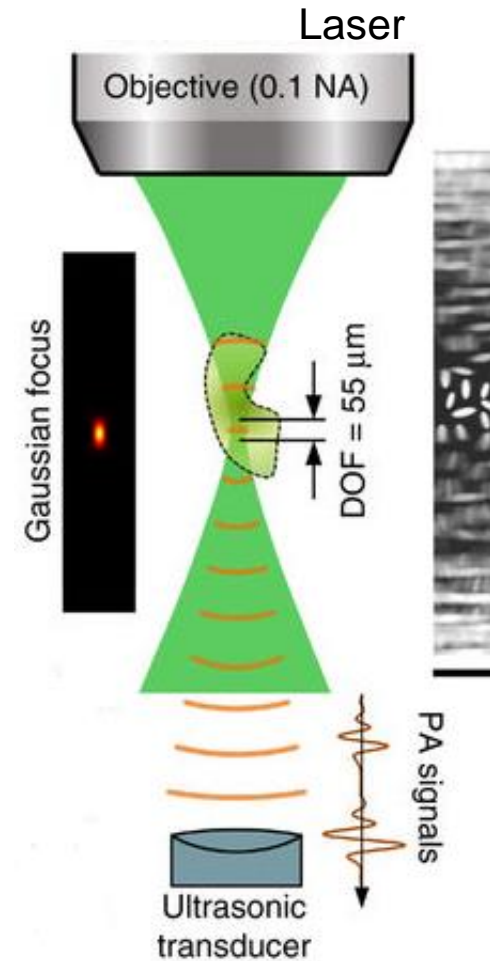
- Photoacoustic (PA) effect is the formation of ultrasound waves following absorption of short laser pulses.
- PA is a rapidly growing research area of hybrid imaging modalities.
- PA imaging combines penetration depth of acoustic waves and high optical resolution.



(a)



(b)



(c)

Fig. 1. Photoacoustic microscopy

2. Compressive Sensing Reconstruction of Photoacoustic images

- **Proposed method**

- The PA signal originates within an area defined by the width of the laser beam.
- Therefore, the actual signal detected by the ultrasound transducer includes multiple PA signals.
- In conventional methods, PA signals are overaged by the focusing lens.
- We propose to use imperfect lens that produces a very complex but deterministic mixing of the input PA signals to the output signal.
- The system of linear equations of PA imaging is given by

$$\mathbf{p} = \mathbf{H}\boldsymbol{\rho}, \quad (1)$$

where $\mathbf{p} \in \mathbb{R}^M$ is the output signal, $\boldsymbol{\rho} \in \mathbb{R}^N$ input PA signal, H transmission matrix which characterizes effect of imperfect lens on PA signal.

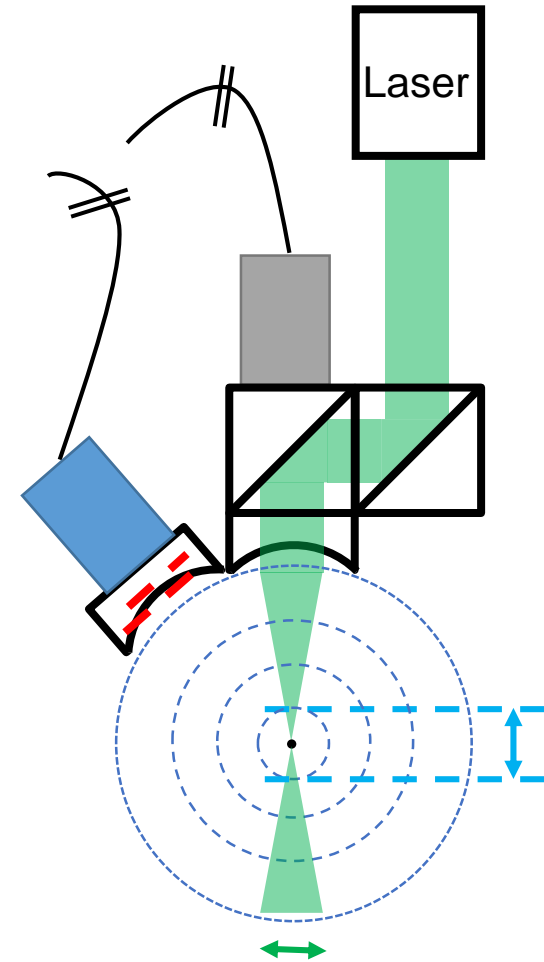


Fig. 2. Photoacoustic microscopy

2. Compressive Sensing Reconstruction of Photoacoustic images

- Simulation

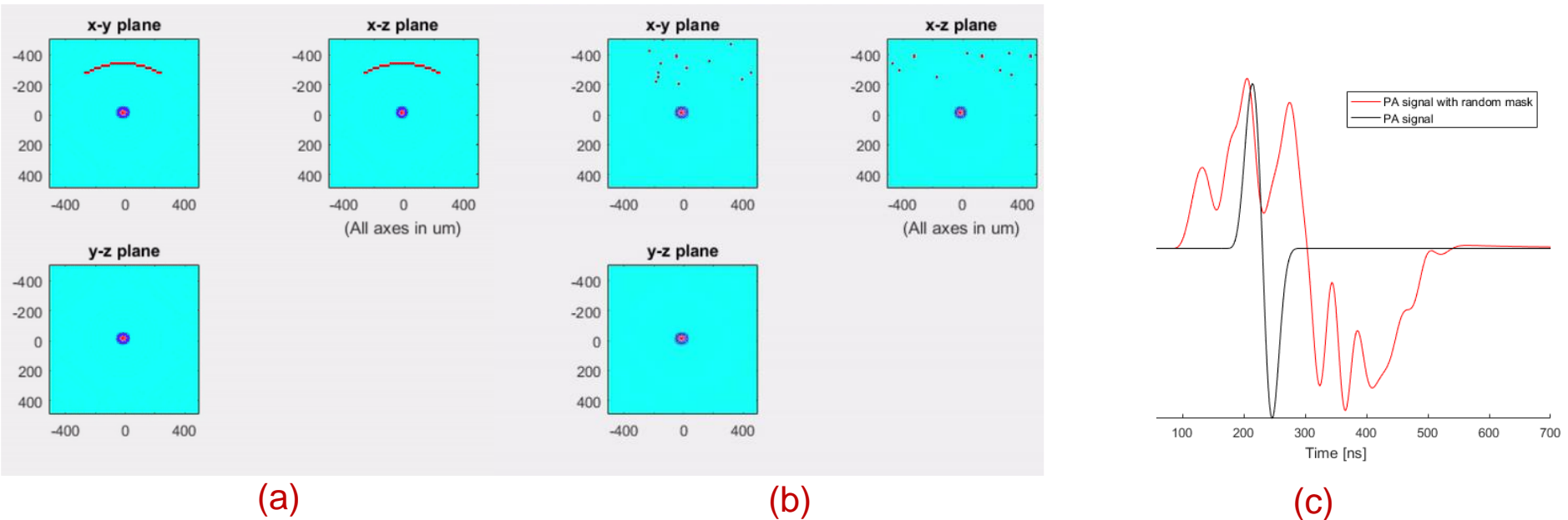
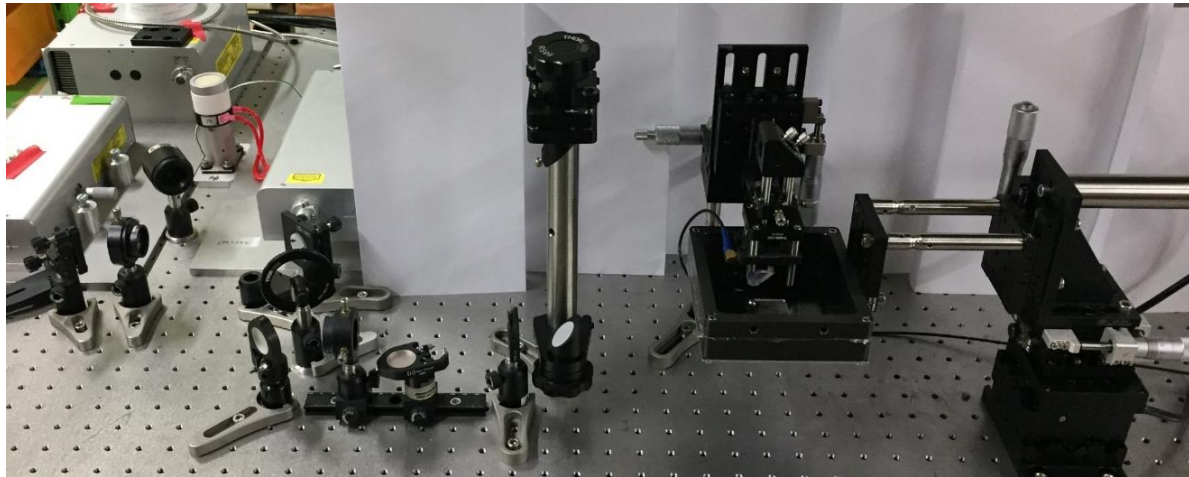


Fig. 3. Simulation results. (a) shows a simulation of the PA signal when conventional concave lens is used. (b) simulation of the PA signal acquired using the proposed imperfect lens. (c) PA signal using conventional lens in black color. And PA signal using imperfect lens is shown in red color.

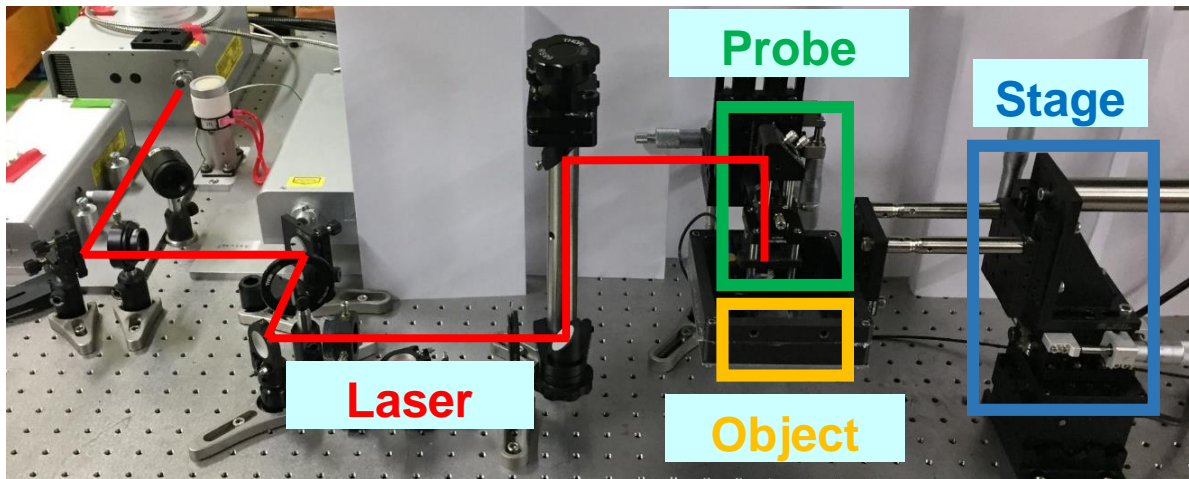
- Conventional PA systems use ideal convex lens to focus acoustic waves in order to achieve perfect PA signal
- In real experiment, due to laser beam width and multiple PA source objects achieving perfect focusing conditions is impossible.

2. Compressive Sensing Reconstruction of Photoacoustic images

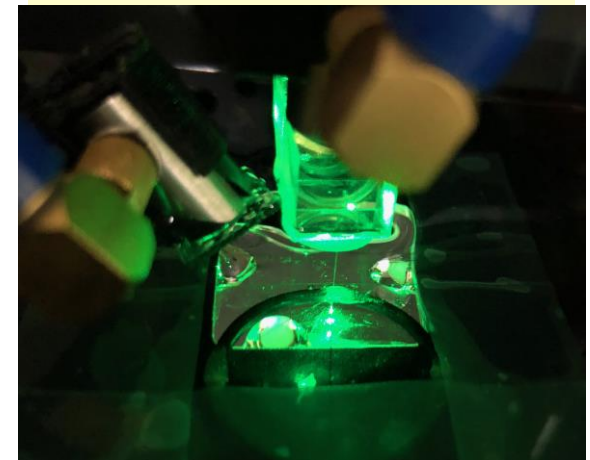
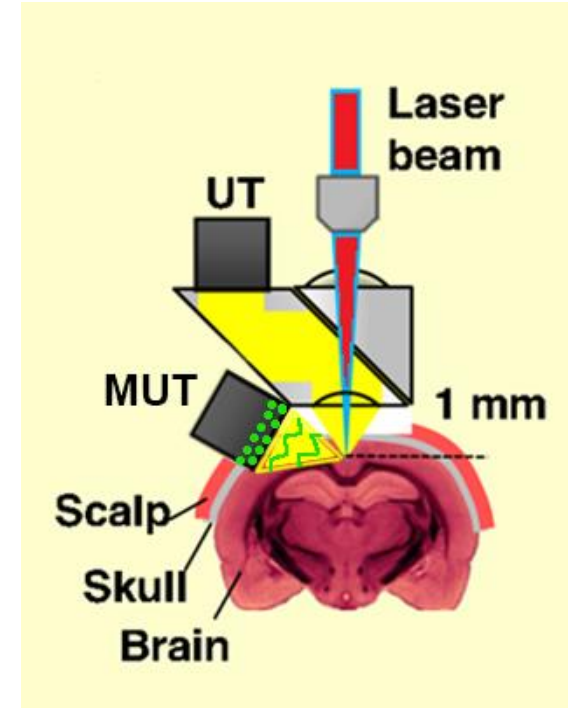
- Research setup



(a)



(b)



(c)

Fig. 4. Photoacoustic microscopy

2. Compressive Sensing Reconstruction of Photoacoustic images

- Results

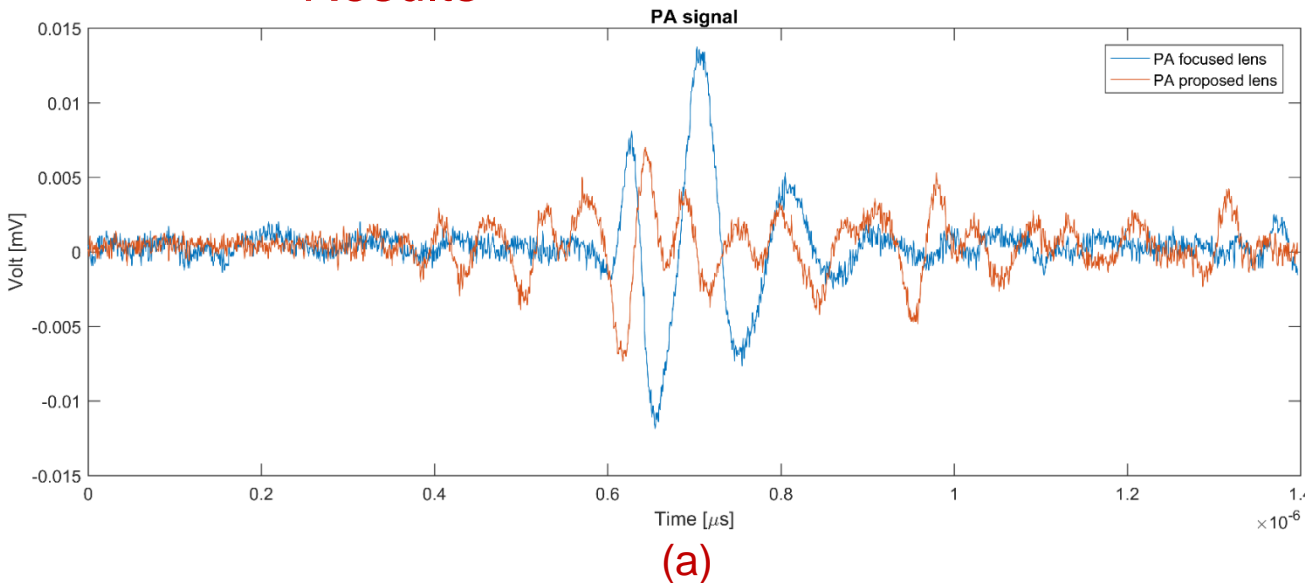
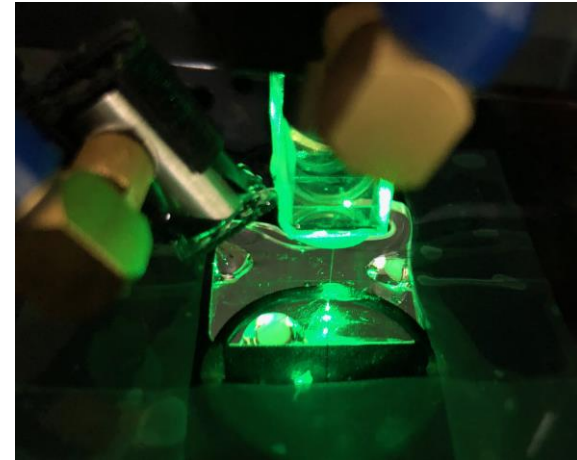


Fig. 5. Photoacoustic experiment. (a) PA signal acquired using focused lens (in blue color), PA signal acquired using proposed imperfect lens (in red color). (b) image of PA setup (c) proposed lens with imperfect surface made by fast curing adhesive

- Modified acoustic lens disturbs the acoustic path of PA signal.
- The received at transducer signal includes multiple PA signals spread in time.
- The acquired PA signal is a function of original PA signal convolved with function of modified acoustic lens



(b)



(c)

2. Compressive Sensing Reconstruction of Photoacoustic images

- Summary

- We propose to intentionally disturb PA signal with imperfect acoustic lens.
- We can create imperfections on lens surface by exposing it to high intensity laser.
- Imperfect lenses can help to improve image resolution of PA systems.
- The transmission matrix of such lenses can be obtained using thorough scanning.

Gwangju Institute of
Science and Technology

School of Electrical Engineering and Computer Science



3. Biomedical Image Processing and Analysis using Deep Neural Networks

3. Biomedical Image Processing and Analysis using Deep Neural Networks

- Introduction

- Deep Learning (DL) or Deep Neural Networks (DNN) allows to significantly improve image reconstruction and image analysis.
- Recently, there is rapidly growing interest in DL methods for biomedical image reconstruction and analysis.
- DNN inspired by the biological neural networks and can be trained to perform different tasks with high accuracy and performance.
- It was already proved in some applications that well trained DL algorithms outperform any previous state of the art methods.
- Today, DL algorithms are mostly used in face/object recognition problems due to availability of large data sets.

3. Biomedical Image Processing and Analysis using Deep Neural Networks

- Introduction

MRI



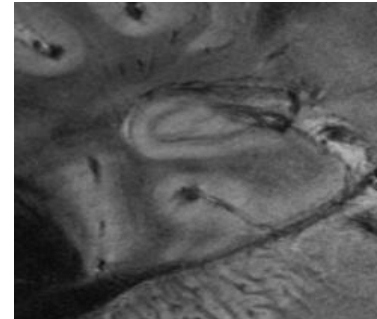
In past

SUPER-RESOLUTION

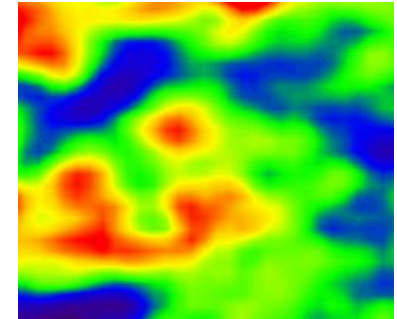


21st century

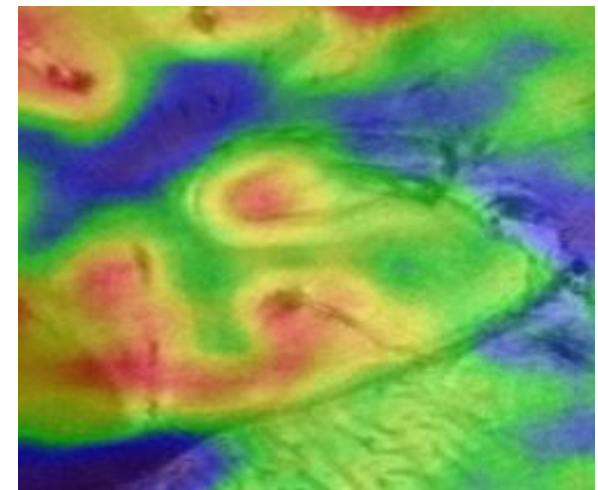
MRI



PET



PET-MRI FUSION



The Future

Fig. 1. Brainstem image

3. Biomedical Image Processing and Analysis using Deep Neural Networks

- Proposed method

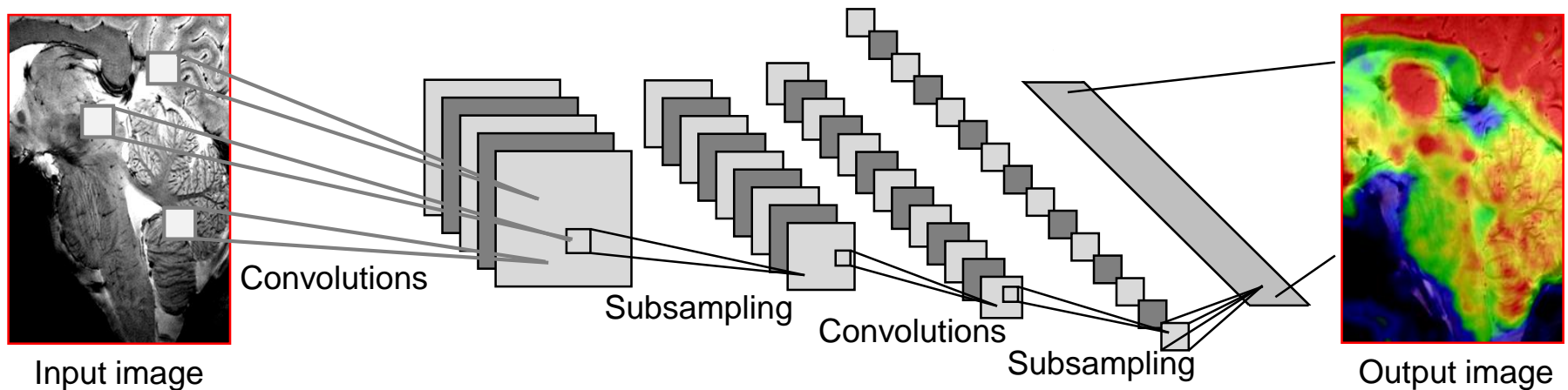
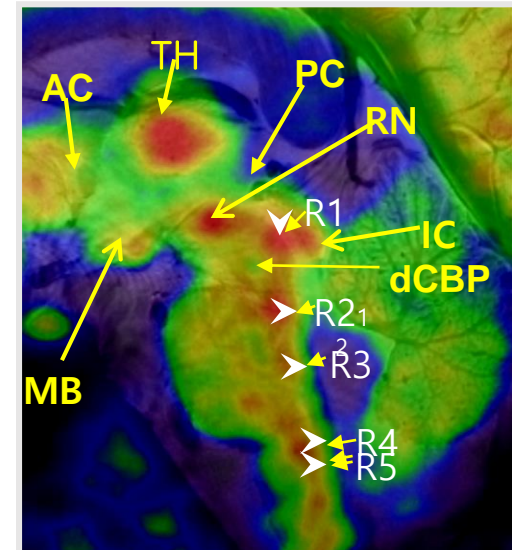


Fig. 2. Proposed DNN for image visualization

- We propose to use DNN to extraction clinically important features from biomedical images
- The proposed DNN will be trained entirely on synthetic data from the simulation software.
- We expect that the proposed DNN will perform with high accuracy on human patients data even if it is trained only on synthetic data.
- Analytical and simulation results will be used to evaluate the advantages or issues of training DNN's on synthetic data



3. Biomedical Image Processing and Analysis using Deep Neural Networks

- Proposed method

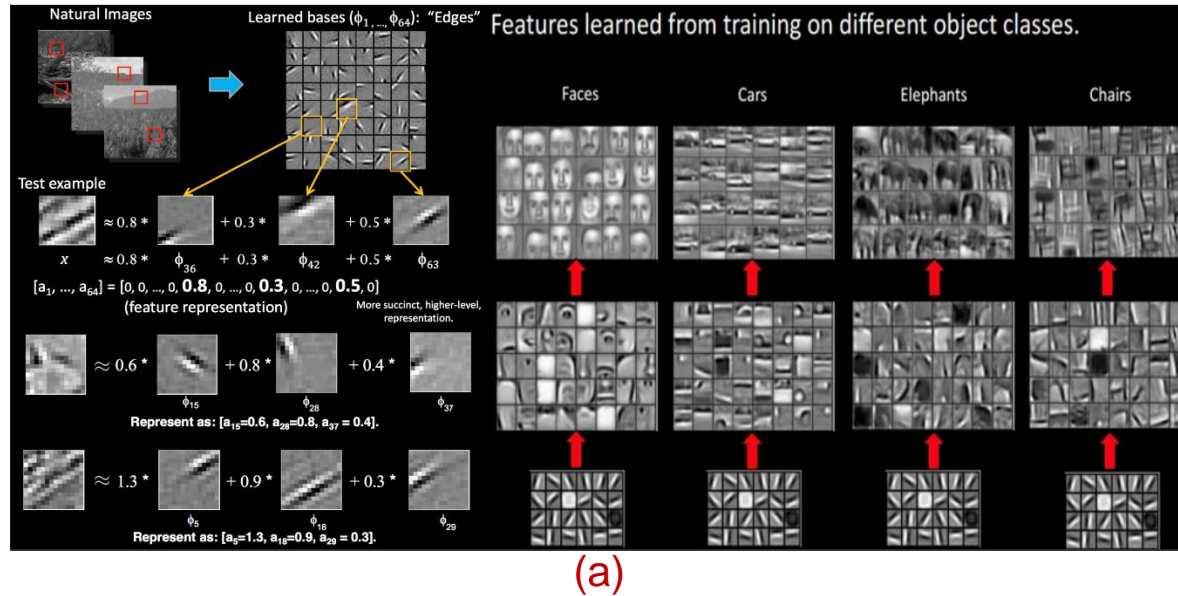


Fig. 3. DNN with application to image recognition

Kernel

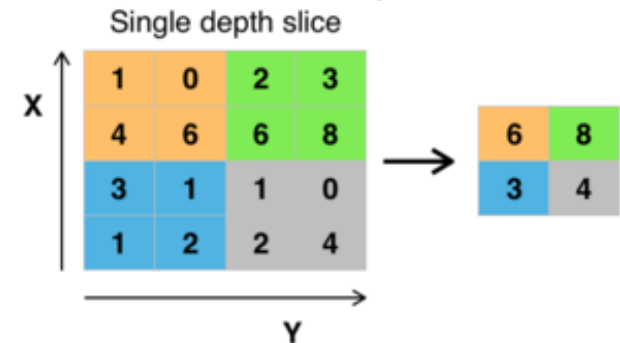
1 _{x1}	1 _{x0}	1 _{x1}	0	0
0 _{x0}	1 _{x1}	1 _{x0}	1	0
0 _{x1}	0 _{x0}	1 _{x1}	1	1
0	0	1	1	0
0	1	1	0	0

4		

Image

Convolved Feature

Max pooling



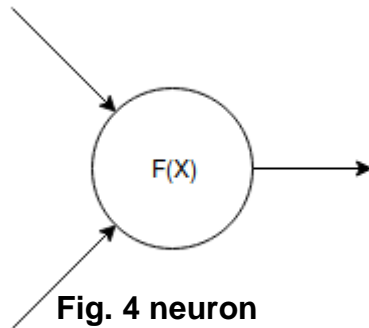
(b)

Ref. LeCun, 2015 & Krizhevsky 2012

- Similar to the DNN in image recognition we can train neural networks to extract meaningful features from biomedical images.
- Backpropagation: at each layer we compute the error with respect to the output class. When the error is known we can adjust network weights (training).

3. Biomedical Image Processing and Analysis using Deep Neural Networks

- Proposed method



- Neuron is a math function that takes several inputs.

$$f(x_1, x_2) = \max(0, w_1x_1 + w_2x_2)$$

here x_k are inputs, for each input neuron assigns weights w_k ,

- The weights are tuned during training session
- The NN is a large number of neurons connected together

- Loss function is a benchmark of how good NN is for a certain task

$$L(y, \hat{y}) = \frac{1}{m} \sum_{i=1}^m (y_i - \hat{y}_i)^2$$

where y is the desired return number from the network, \hat{y} is the actual number network has returned, i is the index of training example.

- In the beginning, NN initialized with random weights.
- During training, we improve Network by changing its weights and minimizing loss function.
- Stochastic Gradient Descent algorithm can be used to optimize function

$$\nabla L \approx \partial \frac{L}{\partial x_i} \nabla x_i$$

- Weights are updated on each step of Gradient function

$$w_j = w_j - lr \partial \frac{L}{\partial x_i}$$

3. Biomedical Image Processing and Analysis using Deep Neural Networks

- Summary

- We propose DNN architecture for biomedical image analysis. The proposed DNN will be train strictly on the synthetic data.
- Also, in this research, we aim to create a open database of synthetic data that can be used by other researches.
- Numerical simulation software such as Field II (ultrasound), k-Wave (photoacoustic), and MRiLab (MRI) will be used to generate large set of labeled data.

Conclusion & Future Work

Conclusion & Future Work

- The already developed Ultrasound Imaging System needs to be fine tuned with the proposed hydrophone experimental setup.
- The proposed compressive sensing Photoacoustic method will be further extended to use random-scattering lenses.
- In the “Image Processing and Analysis using Deep Neural Networks” a final version of network architecture needs to be carefully designed.

Planned manuscript submissions

1. Pavel Ni, Heung-No Lee, “High-Resolution Sonography using Wave Interference”, *IEEE Transactions on Ultrasonics, Ferroelectrics, and Frequency Control*
2. Pavel Ni, Hwi Don Lee, Tae Joong Eom, Heung-No Lee, “Photoacoustic Image Reconstruction using Compressive Sensing”, *IEEE Transactions on Ultrasonics, Ferroelectrics, and Frequency Control*
3. Pavel Ni, Heung-No Lee, “Biomedical Image Processing and Analysis using Deep Neural Networks”, *Sci Rep*

Thank you

Questions and Comments

Appendix A

1. High-Resolution Sonography using Wave Interference

- We can model the received ultrasound signal as

$$p(\mathbf{r}_i, t) = v(t) \underset{t}{\otimes} f(\mathbf{r}_k) \underset{r}{\otimes} h(\mathbf{r}_k, \mathbf{r}_j, \mathbf{r}_i, t) \quad (5)$$

where $v(t)$ is the pulse-echo transducer oscillation

$$v(t) = \frac{\rho}{2c^2} E(t) \underset{t}{\otimes} \frac{\partial^3 w_j(t)}{\partial t^3}, \quad (6)$$

$f(\mathbf{r}_k)$ is the inhomogeneity of the medium

$$f(\mathbf{r}_k) = \frac{\Delta\rho(\mathbf{r}_k)}{\rho_0} - \frac{2\Delta c(\mathbf{r}_k)}{c_0}, \quad (7)$$

$h(\mathbf{r}_k, \mathbf{r}_j, \mathbf{r}_i, t)$ is the pulse-echo spatial impulse response

$$h(\mathbf{r}_k, \mathbf{r}_j, \mathbf{r}_i, t) = \sum_j h_t(\mathbf{r}_k, \mathbf{r}_j, t) \underset{t}{\otimes} h_r(\mathbf{r}_i, \mathbf{r}_k, t) \quad (8)$$

Then the received ultrasound signal is

$$p(\mathbf{r}_i, t) = E_m(t) \underset{t}{\otimes} \frac{1}{2} \int_{V'} F_{op} \left[\sum_{j=0}^{L-1} \rho_0 \frac{\partial w_j(t)}{\partial t} \underset{t}{\otimes} h_t(\mathbf{r}_k, \mathbf{r}_j, t) \right] \underset{t}{\otimes} h_r(\mathbf{r}_i, \mathbf{r}_k, t) d^3 \mathbf{r}_k, \quad (9)$$

$$\mathbf{p}_i = \mathbf{G}_i \mathbf{f}_i, \quad (10)$$

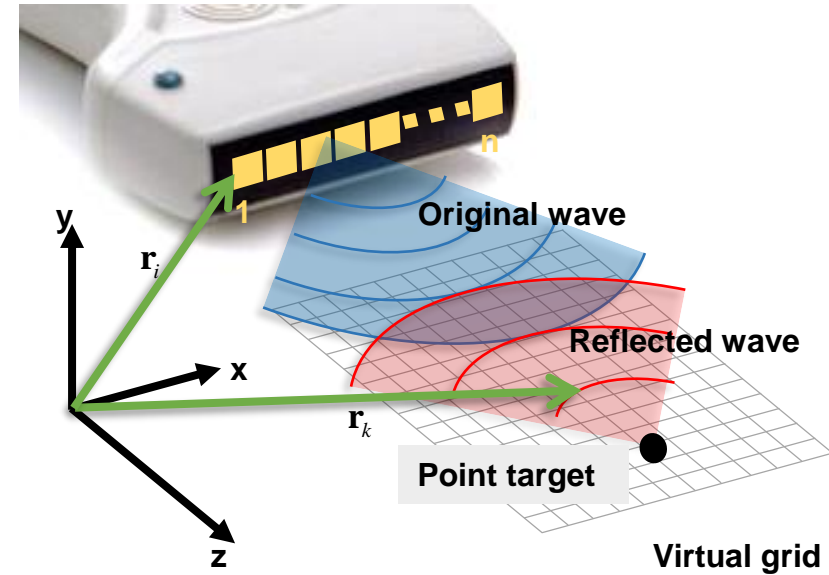


Fig. 7. Sonography

Back >

Appendix B

2. Compressive Sensing Reconstruction of Photoacoustic images

- Modeling PA waves. The equation of motion (conservation of momentum)

$$\frac{\partial}{\partial t} \mathbf{u}(\mathbf{x}, t) = -\frac{1}{\rho_0(\mathbf{x})} \nabla p(\mathbf{x}, t), \quad (1)$$

- The equation of continuity (conservation of mass)

$$\frac{\partial}{\partial t} \rho(\mathbf{x}, t) = -\rho_0(\mathbf{x}) \nabla \cdot \mathbf{u}(\mathbf{x}, t), \quad (2)$$

- The adiabatic equation of state

$$p(\mathbf{x}, t) = c_0(\mathbf{x})^2 \rho(\mathbf{x}, t), \quad (3)$$

- Where $p(\mathbf{x}, t)$ is the acoustic pressure at time $t \in \mathbb{R}^+$ and position $\mathbf{x} \in \Omega \subset \mathbb{R}^n$ inside the imaging region Ω , $\mathbf{u}(\mathbf{x}, t)$ is acoustic particle velocity, $c_0(\mathbf{x})$ is the sound speed, and $\rho(\mathbf{x}, t)$ is acoustic density.

$$p(\mathbf{x}, t) = c_0(\mathbf{x})^2 \left\{ 1 + \tau(\mathbf{x}) \frac{\partial}{\partial t} (-\nabla^2)^{\frac{\gamma}{2}-1} + \eta(\mathbf{x}) (-\nabla^2)^{\frac{\gamma+1}{2}-1} \right\} \rho(\mathbf{x}, t), \quad (4)$$

- Then $p_m(\mathbf{x}_S, t)$ is the signal of pressure $p(\mathbf{x}, t)$ recorded at arbitrary surface $\mathbf{x}_S \in S$ for time $t = (0, \dots, T)$

- The goal is to find estimate of $\rho(\mathbf{x}, t)$

$$\mathbf{p} = \mathbf{H}\rho, \quad (5)$$

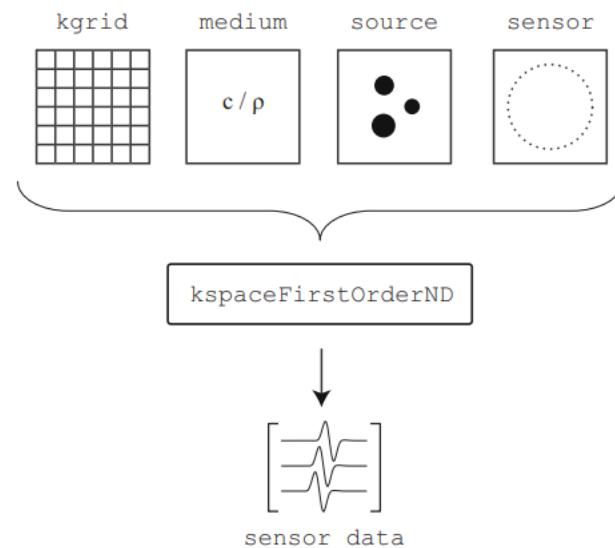


Fig. Photoacoustic simulation

Back >

References

High-Resolution Sonography using Wave Interference

- [1] A. A. Maznev, and O. B. Wright, "Upholding the diffraction limit in the focusing of light and sound," *Wave Motion*, vol. 68, pp. 182-189, 2017/01/01, 2017.
- [2] J. Kang, J. Y. Lee, and Y. Yoo, "A New Feature-Enhanced Speckle Reduction Method Based on Multiscale Analysis for Ultrasound B-Mode Imaging," *IEEE Transactions on Biomedical Engineering*, vol. 63, no. 6, pp. 1178-1191, Jun, 2016.
- [3] P. C. Tay, C. D. Garson, S. T. Acton et al., "Ultrasound Despeckling for Contrast Enhancement," *IEEE Transactions on Image Processing*, vol. 19, no. 7, pp. 1847-1860, Jul, 2010.
- [4] I. Trots, Y. Tasinkevych, A. Nowicki et al., "Golay Coded Sequences in Synthetic Aperture Imaging Systems," *Archives of Acoustics*, vol. 36, no. 4, pp. 913-926, 2011.
- [5] P. Gong, M. C. Kolios, and Y. Xu, "Delay-encoded transmission and image reconstruction method in synthetic transmit aperture imaging," *IEEE Trans Ultrason Ferroelectr Freq Control*, vol. 62, no. 10, pp. 1745-56, Oct, 2015.
- [6] N. Wagner, Y. C. Eldar, A. Feuer et al., "Xampling in ultrasound imaging." p. 17.
- [7] N. Wagner, Y. C. Eldar, and Z. Friedman, "Compressed Beamforming in Ultrasound Imaging," *IEEE Transactions on Signal Processing*, vol. 60, no. 9, pp. 4643-4657, Sep, 2012.
- [8] J. Zhou, S. Hoyos, and B. M. Sadler, "Asynchronous Compressed Beamformer for Portable Diagnostic Ultrasound Systems," *IEEE Transactions on Ultrasonics Ferroelectrics and Frequency Control*, vol. 61, no. 11, pp. 1791-1801, Nov, 2014.
- [9] J. Liu, Q. He, and J. Luo, "A Compressed Sensing Strategy for Synthetic Transmit Aperture Ultrasound Imaging," *IEEE Trans Med Imaging*, vol. 36, no. 4, pp. 878-891, Apr, 2017.
- [10] G. David, J. L. Robert, B. Zhang et al., "Time domain compressive beam forming of ultrasound signals," *J Acoust Soc Am*, vol. 137, no. 5, pp. 2773-84, May, 2015.
- [11] A. Liutkus, D. Martina, S. Popoff et al., "Imaging With Nature: Compressive Imaging Using a Multiply Scattering Medium," *Scientific Reports*, vol. 4, pp. 4052, 07/09/online, 2014.
- [12] P. v. d. M. Pieter Kruizinga*, Andrejs Fedjajevs, Frits Mastik, Geert Springeling, Nico de Jong, Johannes G. Bosch and Geert Leus, "Compressive 3D ultrasound imaging using a single sensor," *Science Advances*, vol. 3, 08 Dec 2017, 2017.
- [13] M. D. Brown, D. I. Nikitichev, B. E. Treeby et al., "Generating arbitrary ultrasound fields with tailored optoacoustic surface profiles," *Applied Physics Letters*, vol. 110, no. 9, Feb 27, 2017.
- [14] B. Lashkari, K. C. Zhang, E. Dovlo et al., "Coded excitation waveform engineering for high frame rate synthetic aperture ultrasound imaging," *Ultrasonics*, vol. 77, pp. 121-132, May, 2017.

References

Compressive Sensing Reconstruction of Photoacoustic Images

- [1] S. Arridge, P. Beard, M. Betcke, B. Cox, N. Huynh, F. Lucka, O. Ogunlade, and E. Zhang. Accelerated high-resolution photoacoustic tomography via compressed sensing. *Phys. Med. Biol.*, 61(24):8908, 2016
- [2] J. Bauer-Marschallinger, K. Felbermayer, and T. Berer. All-optical photoacoustic projection imaging. *Biomed. Opt. Express*, 8(9):3938–3951, 2017.
- [3] P. Burgholzer, J. Bauer-Marschallinger, H. Grün, M. Haltmeier, and G. Paltauf. Temporal back-projection algorithms for photoacoustic tomography with integrating line detectors. *Inverse Probl.*, 23(6):S65–S80, 2007.
- [4] P. Burgholzer, M. Sandbichler, F. Kraemer, T. Berer, and M. Haltmeier. Sparsifying transformations of photoacoustic signals enabling compressed sensing algorithms. *Proc. SPIE*, 9708:970828–8, 2016.
- [5] M. Haltmeier, T. Berer, S. Moon, and P. Burgholzer. Compressed sensing and sparsity in photoacoustic tomography. *J. Opt.*, 18(11):114004–12pp, 2016.
- [6] J. Provost and F. Lesage, The application of compressed sensing for photo-acoustic tomography, *IEEE Transactions on Medical Imaging*, 28 (2009), pp. 585–594
- [7] J. Meng, L. V. Wang, L. Ying, D. Liang, and L. Song, Compressed-sensing photoacoustic computed tomography in vivo with partially known support, *Opt. Express*, 20 (2012), pp. 16510–16523
- [8] T. Mast, L. Souriau, D.-L. Liu, M. Tabei, A. Nachman, and R. Waag, A k-space method for large-scale models of wave propagation in tissue, *Ultrasonics, Ferroelectrics, and Frequency Control*, *IEEE Transactions on*, 48 (2001), pp. 341–354

References

Biomedical Image Processing and Analysis using Deep Neural Networks

- [1] Albarqouni, S., Baur, C., Achilles, F., Belagiannis, V., Demirci, S., Navab, N., 2016. AggNet: deep learning from crowds for mitosis detection in breast cancer histology images. *IEEE Trans. Med. Imaging* 35 (5), 1313–1321
- [2] Chen, H., Dou, Q., Wang, X., Qin, J., Cheng, J.C., Heng, P.-A., 2016. 3D fully convolutional networks for intervertebral disc localization and segmentation. In: *Proceedings of the 2016 International Conference on Medical Imaging and Virtual Reality*. Springer International Publishing, pp. 375–382.
- [3] Chen, H., Dou, Q., Yu, L., Qin, J., Heng, P.-A., 2017. VoxResNet: Deep voxelwise residual networks for brain segmentation from 3D MR images. *NeuroImage*
- [4] Moeskops, P., Viergever, M.A., Mendrik, A.M., de Vries, L.S., Benders, M.J., Išgum, I., 2016a. Automatic segmentation of mr brain images with a convolutional neural network. *IEEE Trans. Med. Imaging* 35 (5), 1252–1261.
- [5] Roth, H.R., Lu, L., Farag, A., Sohn, A., Summers, R.M., 2016. Spatial Aggregation of Holistically-Nested Networks for Automated Pancreas Segmentation. Springer International Publishing, Cham, pp. 451–459.
- [6] Liu, J., Wang, D., Wei, Z., Lu, L., Kim, L., Turkbey, E., Summers, R. M., 2016a. Colitis detection on computed tomography using regional convolutional neural networks. In: *IEEE Int Symp Biomedical Imaging*. pp. 863–866.
- [7] Li, W., Cao, P., Zhao, D., Wang, J., 2016a. Pulmonary nodule classification with deep convolutional neural networks on computed tomography images. *Computational and Mathematical Methods in Medicine*, 6215085.
- [8] Lekadir, K., Galimzianova, A., Betriu, A., Del Mar Vila, M., Igual, L., Rubin, D. L., Fernandez, E., Radeva, P., Napel, S., Jan. 2017. A convolutional neural network for automatic characterization of plaque composition in carotid ultrasound. *IEEE J Biomed Health Inform* 21, 48–40.
- [9] Wang, J. et al. Detecting Cardiovascular Disease from Mammograms with Deep Learning. *IEEE transactions on medical imaging* (2017).
- [10] Ortiz, A., Munilla, J., Gorritz, J. M. & Ramirez, J. Ensembles of Deep Learning Architectures for the Early Diagnosis of the Alzheimer's Disease. *Int J Neural Syst* 26